Uniform approximation for the overlap caustic of a quantum state with its translations

E. Zambrano‡ and A. M. Ozorio de Almeida§

Centro Brasileiro de Pesquisas Físicas, Rua Xavier Sigaud 150, 22290-180, Rio de Janeiro, R.J., Brazil

Abstract.

The semiclassical Wigner function for a Bohr-quantized energy eigenstate is known to have a caustic along the corresponding classical closed phase space curve in the case of a single degree of freedom. Its Fourier transform, the semiclassical chord function, also has a caustic along the conjugate curve defined as the locus of diameters, i.e. the maximal chords of the original curve. If the latter is convex, so is its conjugate, resulting in a simple fold caustic. Indentations in the quantized curve generate self-intersections of the closed fold line and isolated cusp points. The uniform approximation through the fold caustic, that is here derived, describes the transition undergone by the overlap of the state with its translation, from an oscillatory regime for small chords, to evanescent overlaps, rising to a maximum near the caustic. The diameter-caustic for the Wigner function is also treated.

‡ zambrano@cbpf.br
§ ozorio@cbpf.br

1. Introduction

It is often assumed that the Wigner function [1], $W(\mathbf{x})$ in the phase plane $\mathbf{x} = (p, q)$, for a semiclassical WKB state can be approximated by a Dirac δ-function on the corresponding classical closed curve in phase space. This simplest approximation does, indeed, lead to reliable expectation values for smooth classical observables. Nonetheless, it is hopelessly inadequate for the description of delicate interference effects. It is then necessary to resort to more refined semiclassical descriptions for the phase space representations of quantum states, such as Berry's uniform approximation for the Wigner function [2].

Quantum interferences are becoming ever more accessible to experiments related to quantum information, either in quantum optics, atom traps, or other quickly developing technologies (see e.g. [3]). So far, such experiments have only been realized for very simple states, but the interesting theoretical features of the states that are investigated here may be an incentive for further experimental work. A typical interference experiment superposes two modified copies of the same initial state . For instance, in quantum optics, it is easy to achieve the unitary transformation that corresponds to a uniform phase space translation (or displacement). This translated state can then interfere with the original state. In general, the unitary *translation operator*

$$\hat{T}_{\boldsymbol{\xi}} = \exp\left[\frac{i}{\hbar}(\boldsymbol{\xi} \wedge \hat{\mathbf{x}})\right] = \exp\left[\frac{i}{\hbar}(\boldsymbol{\xi}_p \cdot \hat{q} - \boldsymbol{\xi}_q \cdot \hat{p})\right], \tag{1.1}$$

acts on the state $|\psi\rangle$ to produce the new state $|\psi_{\boldsymbol{\xi}}\rangle = \hat{T}_{\boldsymbol{\xi}}|\psi\rangle$ in strict correspondence to the classical translation: $\mathbf{x} \mapsto \mathbf{x} + \boldsymbol{\xi}$. ‖ Thus, given an arbitrary superposition of a state and its translation, $a|\psi\rangle + b|\psi_{\boldsymbol{\xi}}\rangle$, with $|a|^2 + |b|^2 = 1$, the probability that this is measured to be in the untranslated state is $|a + b\langle\psi|\psi_{\boldsymbol{\xi}}\rangle|^2$.

Evidently, measurements of such probabilities (through repeated preparation) supply detailed quantum information concerning these initial states. It so happens that the full set of possible overlaps defines the complete phase space representation,

$$\chi(\boldsymbol{\xi}) = \frac{1}{(2\pi\hbar)}\langle\psi|\hat{T}_{-\boldsymbol{\xi}}|\psi\rangle. \tag{1.2}$$

This is known as the *chord function* [4], the *quantum characteristic function* (or the *Weyl function* as in [5]), which is the Fourier transform of the Wigner function:

$$\chi(\boldsymbol{\xi}) = \frac{1}{(2\pi\hbar)}\int d\mathbf{x}\, W(\mathbf{x}) \exp\left\{\frac{i}{\hbar}(\boldsymbol{\xi} \wedge \mathbf{x})\right\}. \tag{1.3}$$

The latter can be redefined, following Royer [4, 6], as

$$W(\mathbf{x}) = \frac{1}{(\pi\hbar)}\langle\psi|\hat{R}_{\mathbf{x}}|\psi\rangle, \tag{1.4}$$

‖ In the optical context $\hat{T}_{\boldsymbol{\xi}}$ is usually referred to as the *displacement operator* and is expressed in terms of creation and annihilation operators for the harmonic oscillator. This is inconvenient for semiclassical analysis.

where $\hat{R}_{\mathbf{x}}$, the Fourier transform of the translation operators, corresponds classically to the phase space reflection through the point $\mathbf{x}$, i. e. $\mathbf{x}_0 \mapsto 2\mathbf{x} - \mathbf{x}_0$. An important consequence is that the phase space correlations [5, 7], for translational interference,

$$C(\boldsymbol{\xi}) = |\langle\psi|\psi_{\boldsymbol{\xi}}\rangle|^2 = (2\pi\hbar)^2 \int \mathrm{d}\boldsymbol{\eta}\, \mathrm{e}^{\mathrm{i}\boldsymbol{\eta}\wedge\boldsymbol{\xi}/\hbar}\, |\chi(\boldsymbol{\eta})|^2 = (2\pi\hbar)^2 \int \mathrm{d}\mathbf{x}\, \mathrm{W}(\mathbf{x})\, \mathrm{W}(\mathbf{x}-\boldsymbol{\xi})\ , \quad (1.5)$$

coincide with the autocorrelation of the Wigner function itself. A study of interference phenomena using the quantum phase space formalism, besides some properties of phase space distributions can be found in [5].

In the limit of small displacements, $\boldsymbol{\xi} \to 0$, the correlations attain their maximal value, $C(0) = 1$. Increased translations reduce them to an oscillatory regime. We shall be concerned with the correlation of states, whose chord function can be semiclassically approximated by [7, 8]

$$\chi(\boldsymbol{\xi}) = \sum_j\, \alpha_j(\boldsymbol{\xi})\, \mathrm{e}^{i\sigma_j(\boldsymbol{\xi})/\hbar} = \sum_j\, \chi_j(\boldsymbol{\xi})\ , \quad (1.6)$$

where the amplitudes and phases are determined by a classical curve, as will be described in the next section. This is similar to the simplest semiclassical approximation for the Wigner function [2]

$$W(\mathbf{x}) = \sum_j\, a_j(\mathbf{x})\, \mathrm{e}^{iA_j(\mathbf{x})/\hbar} = \sum_j\, W_j(\mathbf{x})\ . \quad (1.7)$$

Furthermore, the Fourier relation between this pair of representations is reflected in the reciprocal relation, which specifies the *centres*

$$\mathbf{x}_j(\boldsymbol{\xi}) = \mathbf{J}\frac{\partial\sigma_j}{\partial\boldsymbol{\xi}}\ , \quad (1.8)$$

for the realizations of the vector $\boldsymbol{\xi}$ as a *chord* of the classical curve, whereas

$$\boldsymbol{\xi}_j(\mathbf{x}) = -\mathbf{J}\frac{\partial A_j}{\partial\mathbf{x}}\ . \quad (1.9)$$

determines the chords that have a given centre. Here,

$$\mathbf{J} = \begin{pmatrix} 0 & -1 \\ 1 & 0 \end{pmatrix} \quad (1.10)$$

is the standard symplectic matrix. Typically for an energy eigenstate, the classical curve is a level curve for the corresponding classical Hamiltonian, related by Bohr-Sommerfeld [9, 10, 11, 12] quantization. In this way (1.6) and (1.7) are alternative phase space representation of WKB wave functions.

For large enough displacements, such that the classical translation of the curve does not intersect the original curve, the phase space correlations are negligible. The transition between this and the previous oscillatory regime takes place along a caustic where the chord function attains locally maximal amplitudes and the simple semiclassical approximation (1.6) breaks down. The main purpose of this paper is to establish the correct description of this transition from the oscillatory regime to the region of negligible overlap through a uniform approximation. It is interesting that the

caustic region for increased quantum correlations is entirely determined by the geometry of the classical curve supporting the quantum state. The simplest case of a convex closed curve is here mostly assumed, so that the locus of its diameters, i.e. its maximal chords, also defines a closed convex curve. However, our results are easily extended to general curves with any number of indentations. The closed caustic curve, will still be generically a fold caustic, except at isolated cusp points, according to Thom's theorem [13]. Though the general method for obtaining uniform approximations can also be extended to these higher singularities, this remains for future work.

The present approximation has some resemblance to the uniform approximation obtained by Berry [2] for the Wigner function close to the classical curve. However, the latter is simplified by symmetry constraints that do not hold here. Indeed, the present treatment is even closer to the uniform approximation along the caustic of the Wigner function far from the curve, which will also be treated. For a start, section 2 reviews the geometrical construction of the Wigner function and the chord function for a state that corresponds to a closed quantized curve. In contrast to the treatment in [2], the construction of the present uniform approximations cannot be limited to a single WKB branch.

Having defined geometrically the stationary phases for the Wigner function and the chord function, the method of Chester, Friedman and Ursell [14] then supplies uniform approximations for the chord function in terms of the Airy function and its derivative in section 3. This treatment is adapted for the diameter caustic of the Wigner function in section 4, except at isolated cusp points that are present even for a convex curve. In both cases, the asymptotic form of these functions for large argument are then connected to the simpler semiclassical forms (1.6) and (1.7). The analysis of these uniform approximations close to the caustic furnishes simpler transitional approximations in section 5.

None of these expressions extends right down to the limit of small chords, because this is another caustic for both the Wigner function and the chord function. However, for the eigenstates of the harmonic oscillator (Fock states), the approximations for large chords can be compared to a small chord formula specified by a Bessel function[7]. This leads to a discussion in section 6 of the normalization of all these phase space approximations, deriving from the limit $C(0) = 1$.

2. Construction of the semiclassical Wigner and chord functions

Before embarking on uniform approximations for the Wigner and chord functions, it is worthwhile to review the derivation of the simpler semiclassical formulae presented in the introduction. Thus we also specify explicitly the amplitudes and phases and their geometric interpretation, which are essential ingredients of the uniform approximations.

The starting point is the generalized WKB expression for the wave function

[9, 10, 11, 12],

$$\langle q|\psi_I\rangle = N\sum_j \left|\frac{\partial^2 S_j(q,I)}{\partial q \partial I}\right|^{\frac{1}{2}} \exp\left[\frac{i}{\hbar}S_j(q,I) + i\beta_j\right]. \tag{2.1}$$

Here we assume that the classical curve is defined as a level curve of the action variable $I(\mathbf{x})$, such that $S_j(q,I)$ corresponds to the j'th branch of the generating function for the canonical transformation $(p,q)\mapsto(I,\theta)$, β_j is the Maslov correction and N is the overall normalization constant. Choosing the arbitrary initial point, q_0, the action branches are defined as

$$S_j(q,I) = \int_{q_0}^{q} p_j(Q,I)\,dQ, \qquad \frac{\partial S_j}{\partial I} = \theta_j, \qquad \frac{\partial S_j}{\partial q} = p_j, \tag{2.2}$$

so that the amplitude can be rewritten in terms of

$$\frac{\partial^2 S_j(q,I)}{\partial q \partial I} = \frac{\partial p_j}{\partial I}(q) = \left[\frac{\partial I}{\partial p}(p_j(q),q)\right]^{-1}. \tag{2.3}$$

It will be assumed that the state corresponds classically to a convex closed curve, so that there will always be a single pair of branches for the action function. This will hold irrespective of any linear canonical transformation, which it may be convenient to make, given that both the chord function and the Wigner functions are covariant with respect to such changes of phase space coordinates. It will also be important to recall that the closed curve must satisfy the Bohr-Sommerfeld quantization condition:

$$\oint p\,dq = 2\pi\hbar\left(n+\frac{1}{2}\right), \qquad n\in\mathbb{Z}. \tag{2.4}$$

Expressing the translation and reflection operators within the position representation (see e.g. [4]), the chord function (1.2) becomes

$$\chi(\boldsymbol{\xi}) = \frac{1}{(2\pi\hbar)}\int dq\,\langle q^+|\psi_I\rangle\,\langle\psi_I|q^-\rangle\,e^{-i\xi_p\cdot q/\hbar} \tag{2.5}$$

while the Wigner (1.4) is given by

$$W(\mathbf{x}) = \frac{1}{(\pi\hbar)}\int d\xi_q\,\langle q^+|\psi_I\rangle\,\langle\psi_I|q^-\rangle\,e^{-ip\cdot\xi_q/\hbar} \tag{2.6}$$

where, in both equations $q^\pm = q \pm \xi_q/2$.

In the semiclassical limit, the WKB expression can be inserted, so that we obtain in each case a sum of integrals that are dominated by their points of stationary phase. Irrespective of whether these points are sufficiently isolated so as to allow for immediate evaluation by the stationary phase method, we need to understand the geometric construction that defines them. In both cases, each stationary point defines values of $q^\pm$ pairs, which are q-coordinates of a pair of points, $\mathbf{x}^\pm$, lying on the classical closed curve. In the case of the chord function, each $\mathbf{x}^-$ is the intersection of the classical curve with its uniform translation by the vector $-\boldsymbol{\xi}$, whereas $\mathbf{x}^+ = \mathbf{x}^- + \boldsymbol{\xi}$. This geometry is exhibited in Fig. 1, which shows that each chord has two *realizations* in a convex closed curve. Thus, this construction on a given convex curve always specifies a pair of centres

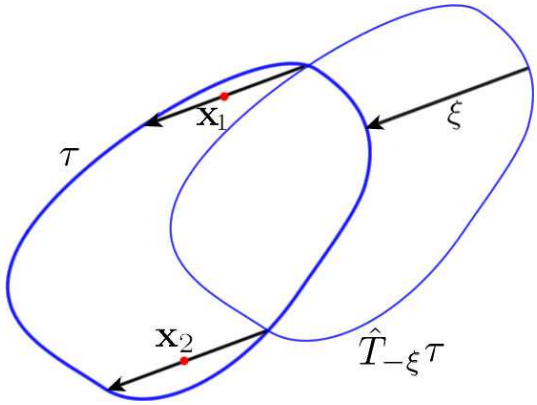

Figure 1. Geometrical construction for the stationary points of the chord function. The intersections at $\mathbf{x}_1{}^-$ and $\mathbf{x}_2{}^-$, of the closed curve with its translation by $-\boldsymbol{\xi}$, define the pair of realizations of this chord. The q-coordinate of the centres, $\mathbf{x}_1$ and $\mathbf{x}_2$ of these realizations defines the stationary points.

$\mathbf{x}_1(\boldsymbol{\xi})$ and $\mathbf{x}_2(\boldsymbol{\xi})$ for each chord $\boldsymbol{\xi}$ that can be fitted in the curve. It should be pointed out that more realizations of a given chord may arise, if we deal with nonconvex curves and, furthermore, such chords may be exterior to the curve. Some of the geometric implications of indentations are discussed in Appendix B, but the important point is that the foregoing theoretical treatment is unaffected, except at singular points.

In the case of the Wigner function, instead of a translation, the classical curve is reflected through the *reflection centre*, $\mathbf{x}$. This results in a pair of intersections, $\mathbf{x}^+$ and $\mathbf{x}^-$, such that $\mathbf{x}$ is the centre for the pair of chords $\boldsymbol{\xi} = \pm(\mathbf{x}^+ - \mathbf{x}^-)$. The stationary points are then the q-coordinates for this pair of chords. This geometry is shown in Fig. 2. Therefore, there will be at least one pair of chords $\pm\boldsymbol{\xi}(\mathbf{x})$, for each reflection centre in the curve.

The stationary phase evaluation of each integral for the Wigner function,

$$W_{ij}(\mathbf{x}) = \frac{N^2}{2\pi\hbar}\int d\xi_q \left|\frac{\partial I}{\partial p}(p_i(q^+), q^+)\frac{\partial I}{\partial p}(p_j(q^-), q^-)\right|^{\frac{1}{2}} \times \exp\left[\frac{i}{\hbar}\left[S_i(q^+, I) - S_j(q^-, I) - p\cdot\xi_q + \beta_i - \beta_j\right]\right], \tag{2.7}$$

can usually be obtained from a single branch of the action function for the closed curve, that is, $i = j$. The stationary phase is half of the area between the curve and its reflection, or the "chord area" as shown in Fig. 2, except for a Maslov correction. The only difference between both phases, corresponding to $\pm\boldsymbol{\xi}(\mathbf{x})$, is the sign, so that the semiclassical approximation is real [2].

In the case of the chord function, each stationary phase is given by the construction in Fig. 3. Unlike the Wigner function, this depends explicitly on a change of phase space origin, $\mathbf{x} \mapsto \mathbf{x} + \boldsymbol{\xi}'$, according to the exact formula [7],

$$\chi_{\boldsymbol{\xi}'}(\boldsymbol{\xi}) = e^{\frac{i}{\hbar}\boldsymbol{\xi}'\wedge\boldsymbol{\xi}}\,\chi(\boldsymbol{\xi}), \tag{2.8}$$

but it is also covariant with respect to homogeneous linear canonical transformations.

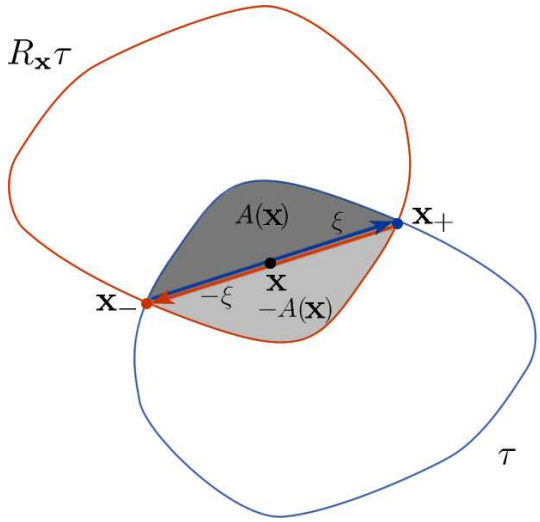

Figure 2. Geometrical construction for the stationary points of the Wigner function. The intersections of the closed curve with its reflection through $\mathbf{x}$ defines pair of chords centred on $\mathbf{x}$. The q-coordinate of these chords defines the stationary points. The area $A(\mathbf{x})$ determines the phase of the Wigner function.

The amplitudes in the above semiclassical approximations are best expressed in terms of the canonical action variable, $I(\mathbf{x})$, that defines the closed curve and is conjugate to the angle variable $\theta(\mathbf{x})$ along the curve. If we now define the transported action variable,

$$I^{\pm} = I(\mathbf{x} \pm \boldsymbol{\xi}/2), \tag{2.9}$$

then, generally, the Poisson bracket for this pair of functions,

$$\{I^+, I^-\} = \frac{\partial I^+}{\partial \mathbf{x}} \wedge \frac{\partial I_-}{\partial \mathbf{x}} \neq 0, \tag{2.10}$$

and it is found that these amplitudes in (1.6) and (1.7) are

$$a(\mathbf{x}) = |\{I^+, I^-\}|^{-\frac{1}{2}} = \alpha(\boldsymbol{\xi}). \tag{2.11}$$

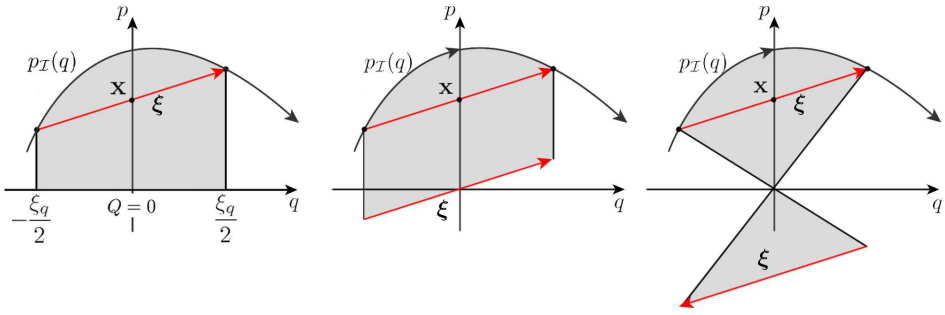

Figure 3. Several geometrical interpretations for the phase for the semiclassical chord function in the simpler approximation for a WKB function, considering one branch. The stationary phase itself is determined by the shaded area in the three cases[7].

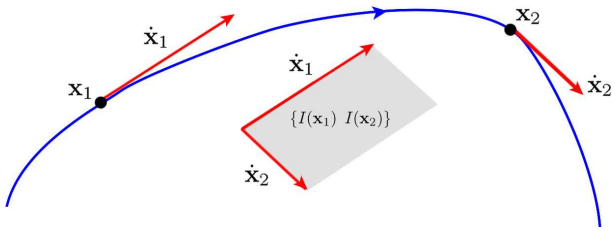

Figure 4. Geometrical interpretation for the semiclassical amplitudes of both the Wigner function and the chord function.

The difference between considering the amplitude as a function on $\mathbf{x}$ or $\boldsymbol{\xi}$ depends on which variable is fixed in (2.11). This only changes the sign of the Poisson bracket. Here, the equality of coefficients for both representations holds for the chord and its centre, between a specific pair of points $(\mathbf{x}^-, \mathbf{x}^+)$ on the closed curve.

A neat interpretation for these amplitudes follows from the identification of the action variable $I(\mathbf{x})$ with a classical Hamiltonian. Then the closed curve becomes a closed trajectory, tangent to the phase space velocity vector, $\dot{\mathbf{x}}$, and

$$\{I^-, I^+\} = \dot{\mathbf{x}}^- \wedge \dot{\mathbf{x}}^+, \tag{2.12}$$

as shown in Fig. 4. It follows that the amplitudes $\alpha_j(\boldsymbol{\xi})$ (or $a_j(\mathbf{x})$), depend on the degree of transversality of the intersection between the curve and its translation, or its reflection [2, 7] and so they diverge at caustics, where $\dot{\mathbf{x}}^+$ and $\dot{\mathbf{x}}^-$ are parallel.

So far, we have presumed that the contribution of each stationary phase point to the integrals for either the Wigner function or the chord function, can be obtained by considering a single branch of the WKB wave function. Thus, $i = j$ in (2.7) and this single branch can always be accessed through a canonical phase space rotation in the simple semiclassical approximations above and even for Berry's uniform theory for the caustic that arises in the limit of small chords [2]. However, this is not possible in the present treatment of the caustic at maximal chords, where (2.11) also diverges for both representations, because the tips of the stationary chord become turning points for the WKB function in this limit. It is thus necessary to study this limit with the aid of phase space coordinates, such that it is the cross term between the pair of different branches, of the action function, which have stationary phases in (2.7). For this reason it will be important to take care of the phase relation between the branches across a turning point:

$$\begin{aligned}\langle q|\psi_I\rangle \ = N \Bigg[\left|\frac{\partial^2 S_+(q,I)}{\partial q \partial I}\right|^{\frac{1}{2}} \exp\left[\frac{i}{\hbar} S_+(q,I)\right] \\ + \mathrm{e}^{i\pi/2} \left|\frac{\partial^2 S_-(q,I)}{\partial q \partial I}\right|^{\frac{1}{2}} \exp\left[\frac{i}{\hbar} S_-(q,I)\right] \Bigg], \end{aligned} \tag{2.13}$$

where $\pi/2$ is the Maslov phase and N is the normalization constant. Inserting the above wave function in (2.5), we obtain four integrals to evaluate. An appropiate choice of the coordinate axes orientation, in which the both of chord realizations are crossed, reduces

the chord function for (2.13) to the single integral

$$\chi(\boldsymbol{\xi}) = \frac{N^2}{2\pi\hbar}\int dq \left|\frac{\partial I}{\partial p}(p_+(q^+),q^+)\frac{\partial I}{\partial p}(p_-(q^-),q^-)\right|^{\frac{1}{2}} \times \exp\left(\frac{i}{\hbar}\left[S_+(q^+,I) - S_-(q^-,I) - \xi_p\cdot q\right] + i\frac{\pi}{2}\right). \qquad (2.14)$$

Here $q^\pm = q \pm \xi_q/2$. As stated previously, this geometry can be guaranteed by a phase space rotation. The evaluation of the chord areas in the Wigner function and the chord function for this geometry is discussed in Appendix A.

3. Uniform approximation for the chord function

Let us allow the pair of these stationary points of (2.14) to coalesce for the chord $\boldsymbol{\xi}_D$, that corresponds to a *diameter* of the closed curve, i.e. a maximal chord, at which the semiclassical amplitude (2.11) diverges. In the present case of a convex curve, these diameters are the locus of a fold caustic with no higher singularity. This is simpler than the geometry for the corresponding caustic of the Wigner function, studied in the following section.

We also simplify the calculation by an appropriate choice of origin, in view of the simple translation property (2.8) of the chord function. This ideal origin lies midway between the centres for the pair of chord realizations, shown in Fig. 5. The pair of stationary points q_1 and q_2 of the integrand in (2.14) are solutions of the equation:

$$p_+(q+\xi_q/2) - p_-(q-\xi_q/2) = \xi_p, \qquad (3.1)$$

which are identified as the position coordinates of $\mathbf{x}_1$ and $\mathbf{x}_2$ in Fig. 5. According to Appendix A, the Bohr-Sommerfeld quantization rule (2.4) leads to the corresponding

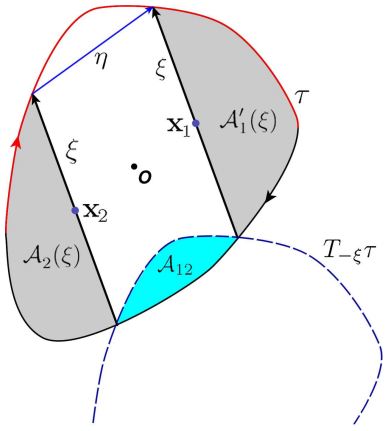

Figure 5. The difference in chord areas, $\mathcal{A}_{12}$, coincides with the area between the closed curve and its translation. This area shrinks to zero when $\boldsymbol{\xi}$ becomes a diameter and its conjugate chord $\boldsymbol{\eta} = \mathbf{x}_1 - \mathbf{x}_2 \to 0$. The simplest choice of phase space origin is at midpoint between $\mathbf{x}_1$ and $\mathbf{x}_2$.

phases as

$$S_+(q_1+\xi_q/2)-S_-(q_1-\xi_q/2)-\xi_p q_1=\mathcal{A}_1(\xi)+\mathbf{x}_1\wedge\boldsymbol{\xi}, \tag{3.2}$$

$$S_+(q_2+\xi_q/2)-S_-(q_2-\xi_q/2)-\xi_p q_2=\mathcal{A}_2(\xi)+\mathbf{x}_2\wedge\boldsymbol{\xi}. \tag{3.3}$$

Instead of evaluating (2.14) by stationary phase, this integral is mapped onto the standard form for a *fold diffraction catastrophe* [15]:

$$\chi(\boldsymbol{\xi})=\frac{N^2}{2\pi i\hbar}\exp\left(\frac{i\Sigma\mathcal{A}}{2\hbar}\right)\int_{-\infty}^{\infty}du\;g(u;\boldsymbol{\xi})\;e^{i\left[\frac{u^3}{3}-\zeta\,u\right]}, \tag{3.4}$$

where we have defined

$$\Sigma\mathcal{A}=\mathcal{A}_1+\mathcal{A}_2,\qquad \frac{2}{3}\zeta(\boldsymbol{\xi})^{\frac{3}{2}}=\frac{\mathcal{A}_{12}}{2\hbar}=\frac{\mathcal{A}_1-\mathcal{A}_2+\boldsymbol{\eta}\wedge\boldsymbol{\xi}}{2\hbar}. \tag{3.5}$$

The action difference, $\mathcal{A}_{12}$, is the main ingredient in the present application of the method of uniform approximation [14, 15]. Its geometric definition is the area between the closed curve and its translation, as shown in Fig. 5. At the caustic, the chord $\boldsymbol{\xi}=\boldsymbol{\xi}_D$ is maximal and its *conjugate chord* [7]: $\boldsymbol{\eta}=\mathbf{x}_1-\mathbf{x}_2\to 0$.

The above integral would define an Airy function [17], $\mathrm{Ai}(\zeta)$, if $g(u;\boldsymbol{\xi})=1$, but here the mapping between the variables $q\mapsto u$, respectively in (2.14) and (3.4), leads to

$$g(u;\boldsymbol{\xi})=\left|\frac{\partial I}{\partial p}(q(u)+\xi_q/2)\frac{\partial I}{\partial p}(q(u)-\xi_q/2)\right|^{-\frac{1}{2}}\frac{dq}{du}. \tag{3.6}$$

The approximation now consists in replacing this by a linear function which coincides with $g(u;\boldsymbol{\xi})$ at the stationary points, $\pm\zeta^{\frac{1}{2}}$ of (3.4). These map onto $q(\zeta^{\frac{1}{2}})=\mathbf{x}_{1q}\equiv q_1$ and $q(-\zeta^{\frac{1}{2}})=\mathbf{x}_{2q}\equiv q_2$. The Jacobian of the mapping $q\leftrightarrow u$ at the stationary points is specified by

$$\frac{dq}{du}(\zeta^{\frac{1}{2}}) \;=\; \left|\frac{2\hbar\zeta^{\frac{1}{2}}}{\frac{\partial p}{\partial q}(q_1+\xi_q/2)-\frac{\partial p}{\partial q}(q_1-\xi_q/2)}\right|^{\frac{1}{2}}, \tag{3.7}$$

$$\frac{dq}{du}(-\zeta^{\frac{1}{2}}) = \left|\frac{2\hbar\zeta^{\frac{1}{2}}}{\frac{\partial p}{\partial q}(q_2+\xi_q/2)-\frac{\partial p}{\partial q}(q_2-\xi_q/2)}\right|^{\frac{1}{2}}, \tag{3.8}$$

so that

$$g(\zeta^{\frac{1}{2}};\boldsymbol{\xi})=\left|\frac{2\hbar\zeta^{\frac{1}{2}}}{\{I_1^+,I_1^-\}}\right|^{\frac{1}{2}},\quad g(-\zeta^{\frac{1}{2}};\boldsymbol{\xi})=\left|\frac{2\hbar\zeta^{\frac{1}{2}}}{\{I_2^+,I_2^-\}}\right|^{\frac{1}{2}}. \tag{3.9}$$

Thus, recalling the definition of the transported action (2.9) for each chord realization, we now define

$$\Delta I^{12}\equiv\left|\{I_1^+,I_1^-\}\right|^{-\frac{1}{2}}-\left|\{I_2^+,I_2^-\}\right|^{-\frac{1}{2}}\quad\text{and}\quad \Sigma I^{12}\equiv\left|\{I_1^+,I_1^-\}\right|^{-\frac{1}{2}}+\left|\{I_2^+,I_2^-\}\right|^{-\frac{1}{2}}, \tag{3.10}$$

so as to obtain

$$g(u;\boldsymbol{\xi})\simeq\sqrt{\frac{\hbar}{2}}\left(\zeta^{\frac{1}{4}}\Sigma I^{12}+\frac{u}{\zeta^{\frac{1}{4}}}\Delta I^{12}\right), \tag{3.11}$$

as an approximation to (3.6), which is linear with respect to u and has the correct values at the stationary points. Thus, the integral for the chord function becomes

$$\chi(\boldsymbol{\xi}) = \frac{N^2}{ih}\frac{\sqrt{\hbar}}{\sqrt{2}}\exp\left(i\frac{\Sigma\mathcal{A}}{2\hbar}\right)\int_{-\infty}^{\infty}du\,\left(\zeta^{\frac{1}{4}}\Sigma I^{12}+\frac{u}{\zeta^{\frac{1}{4}}}\Delta I^{12}\right)e^{i\left[\frac{u^3}{3}-\zeta\,u\right]} \quad (3.12)$$

$$= \frac{N^2}{i}\frac{1}{\sqrt{2\hbar}}\exp\left(i\frac{\Sigma\mathcal{A}}{2\hbar}\right)\left(\zeta^{\frac{1}{4}}\Sigma I^{12}\mathrm{Ai}\left(-\zeta\right)-\frac{i}{\zeta^{\frac{1}{4}}}\Delta I^{12}\mathrm{Ai}'\left(-\zeta\right),\right) \quad (3.13)$$

where Ai' is the derivative of the Airy function. Finally, recalling the definition of the intermediate variable, ζ, in terms of areas (3.5), we obtain the full unitary approximation for the chord function:

$$\chi(\boldsymbol{\xi}) \;= N^2\exp\left(i\frac{\Sigma\mathcal{A}}{2\hbar}\right)\left[\frac{\left[\frac{3}{4}\mathcal{A}_{12}\right]^{\frac{1}{6}}\Sigma I^{12}}{i\sqrt{2}\hbar^{\frac{2}{3}}}\mathrm{Ai}\left(-\left[\frac{3\mathcal{A}_{12}}{4\hbar}\right]^{\frac{2}{3}}\right)\right.$$

$$\left.-\,\frac{\left[\frac{3}{4}\mathcal{A}_{12}\right]^{-\frac{1}{6}}\Delta I^{12}}{\sqrt{2}\hbar^{\frac{1}{3}}}\mathrm{Ai}'\left(-\left[\frac{3\mathcal{A}_{12}}{4\hbar}\right]^{\frac{2}{3}}\right)\right]. \quad (3.14)$$

The Airy function, $\mathrm{Ai}\left(-\zeta\right)$, oscillates with increasing amplitude as its argument increases and then decays exponentially for positive values of $-\zeta$. The maximum amplitude attained by this function, just bellow the origin, indicates the singularity of the simple semiclassical amplitude at the caustic. However, this uniform approximation (3.14) is not yet explicitly resolved very close to the caustic, because $\mathcal{A}_{12}\to 0$ as the caustic is approached, whereas $\Sigma I^{12}\to\infty$. This undeterminacy will be fully resolved in section 5.

Even so, it is clear that the second term depending on $\mathrm{Ai}'\left(-\zeta\right)$ can be neglected in the region close to the caustic. It is a new feature in comparison with the uniform approximation for the Wigner function for small chords [2], where it is absent because of the reflection symmetry. Here, this term is essential to obtain the correct limiting behaviour in the oscillatory region, where the simple semiclassical description is valid. The other novel feature is the oscillatory phase proportional to $\Sigma\mathcal{A}$ along the caustic, which will be important to separate the contribution of each realization at the oscillatory regime. Indeed in the case when the chord areas are significantly greater than Planck's constant, the functions in (3.14) can be replaced by the asymptotic forms for large negative values [17],

$$\mathrm{Ai}(-\zeta)\to\frac{1}{\sqrt{\pi}\zeta^{\frac{1}{4}}}\cos\left(\frac{2}{3}\zeta^{\frac{3}{2}}-\frac{\pi}{4}\right)\quad\text{and}\quad\mathrm{Ai}'(-\zeta)\to\frac{\zeta^{\frac{1}{4}}}{\sqrt{\pi}}\sin\left(\frac{2}{3}\zeta^{\frac{3}{2}}-\frac{\pi}{4}\right), \quad (3.15)$$

in order to obtain the correct form in the oscillatory regime as in (1.6):

$$\chi(\boldsymbol{\xi})\to\frac{N^2}{i\sqrt{2\pi\hbar}}\left[\frac{\exp\left(i\left[\frac{\mathcal{A}_1}{\hbar}-\frac{\pi}{4}\right]\right)}{|\{I_1^+,I_1^-\}|^{\frac{1}{2}}}+\frac{\exp\left(i\left[\frac{\mathcal{A}_2}{\hbar}+\frac{\pi}{4}\right]\right)}{|\{I_2^+,I_2^-\}|^{\frac{1}{2}}}\right]. \quad (3.16)$$

This result corresponds to the sum of contributions for each chord realization in the simpler stationary phase approximation of the semiclassical chord function in [7], where

it was considered that each chord realization lies on a single branch of the WKB wave function.

Finally, we point out that the assumption of convexity for the quantized curve can be relaxed. This arises naturally as a constant energy curve for a double well, or from the classical evolution of a convex curve, if the original curve did not have constant energy. The corresponding semiclassical WKB states are then defined in the same way as above, but the action will have a larger number of branches. It is shown in Appendix B that there may then appear regions in chord space with more than two chord realizations. The locus of diameters is still a caustic line, acting as a boundary for the different regions, but now it may exhibit self-intersections at double fold points, as well as cusp points. Far from the caustic, each chord realization contributes an oscillatory exponential term to the chord function, of the same form as those in (3.16), which could be obtained directly from (2.14) by the method of stationary phase. Close to the fold line, we must substitute the pair of contributions which coalesce there by the corresponding uniform approximation, as described above. This is possible even at a double fold point, or if the centre of the chord is exterior to the quantized curve.

According to Thom's theorem [13], cusp points are the only other generic singularity to arise on the diameter caustic. The above theory breaks down at such points, because they correspond to the coalescion of a triplet of chords. However, the same general approach can in principle be carried out by mapping the integrals onto the corresponding higher *diffraction catastrophe*, as described by Berry in [15].

4. Uniform approximation for the Wigner function

As the Wigner function is evaluated at a point $\mathbf{x}$ that lies further and further inside a convex closed classical curve, a caustic will be crossed. This is typically a cusped triangle[2], in which there are three chords for each centre, as shown in Fig. 6. Typical paths to its interior enter the triangle through a fold caustic joining two cusps. Such a caustic point $\{\mathbf{x}_i\}$ is the centre of a diameter, as show in Fig. 6, as well as being the centre of the other chord, which was followed in the continuous path through the caustic. An example of the full fringe pattern, where the regions characterized by one or three chords are clearly discernible, can be found in [8].

Again, invoking Thom's theorem, we can safely limit the generic effect of indentations of the quantized curve on the diameter caustic to a greater number of cusp points and self intersections. The fold line is always the boundary between regions with different numbers of chords. It should be recalled that *generic* implies a structural stability with respect to perturbations (of the shape of the classical curve). In particular, a curve with a centre of (reflection) symmetry, such as a circle or an ellipse, is highly ungeneric, because this point is the centre of an infinite number of chords, so that the diameter caustic collapses to a point. As discussed in [7], the class of centro-symmetric states are notable in that their Wigner and chord functions are related by a

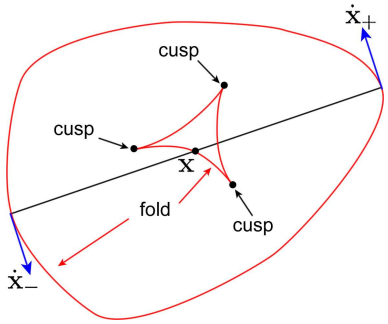

Figure 6. Wigner function caustic for a quantized closed curve. The curve itself is a fold caustic (*short-chord catastrophe*). Another singular curve, composed of folds and cusps (*the diameter caustic*), lies in the interior of the quantized curve. These catastrophe points correspond to centres of the diameters of the outer curve. Indentations of the quantized curve may increase the number of cusp points, or add self-intersections to the diameter caustic.

mere rescaling. ¶

The uniform approximation to be derived here concerns the pair of chords, $\boldsymbol{\xi}_1$ and $\boldsymbol{\xi}_2$ in Fig. 7, that are born from the diameter at the caustic. Away from the cusps, the contribution of the separate chord, $\boldsymbol{\xi}_3$ in Fig. 7, can still be evaluated by stationary phase. This is just a simple semiclassical contribution,

$$W_3(\mathbf{x}) = \frac{4N^2}{\sqrt{\hbar}} \left|\{I(\mathbf{x}+\boldsymbol{\xi}_3/2), I(\mathbf{x}-\boldsymbol{\xi}_3/2)\}\right|^{-\frac{1}{2}} \cos\left(\frac{A_3}{\hbar} - \frac{\pi}{4}\right), \tag{4.1}$$

which could be obtained from a single WKB branch, $i = j$ in (2.7). This could also be derived from a cross-branch $i \neq j$ (by rotating the phase space coordinates) from the same integral that furnishes the joint contribution of the pair of chords, $\boldsymbol{\xi}_1$ and $\boldsymbol{\xi}_2$, which coalesce at the diameter $\boldsymbol{\xi}_D$.

This crossed chord picture is essential for the uniform approximation. As in the theory for the chord function, we now map the integral in the region corresponding to the chords $\boldsymbol{\xi}_1$ and $\boldsymbol{\xi}_2$ onto the diffraction integral, as in (3.4).

$$W(\mathbf{x}) = 2\Re\mathfrak{e}\frac{N^2}{i2\pi\hbar}\exp\left(i\frac{\Sigma A}{2\hbar}\right)\int_{-\infty}^{\infty} dz\, g(z;\mathbf{x})\, e^{i\left[\frac{z^3}{3}-\zeta z\right]} + W_3(\mathbf{x}). \tag{4.2}$$

Here the parameters of the transformation are given by

$$\Sigma A = A_1(\mathbf{x}) + A_2(\mathbf{x}), \qquad \frac{2}{3}\zeta^{\frac{3}{2}}(\mathbf{x}) = \frac{A_{12}(\mathbf{x})}{2\hbar} = \frac{A_1(\mathbf{x}) - A_2(\mathbf{x})}{2\hbar}, \tag{4.3}$$

in which A_{12} is the symplectic area bounded by the closed curve and its reflection between the ends of $\boldsymbol{\xi}_1$ and $\boldsymbol{\xi}_2$, as show Fig. 7. The procedure is straightforward as for the chord function, so that recalling that $I_j^{\pm}(\mathbf{x}) = I(\mathbf{x} \pm \boldsymbol{\xi}_j/2)$, we now define

$$\Delta I_{12} \equiv \left|\{I_1^+, I_1^-\}\right|^{-\frac{1}{2}} - \left|\{I_2^+, I_2^-\}\right|^{-\frac{1}{2}} \quad \text{and} \quad \Sigma I_{12} \equiv \left|\{I_1^+, I_1^-\}\right|^{-\frac{1}{2}} + \left|\{I_2^+, I_2^-\}\right|^{-\frac{1}{2}}. \tag{4.4}$$

¶ However, the ungeneric point-caustic of the chord function determines the limit of short chords and it is structurally stable even for states lacking a reflection stmmetry.

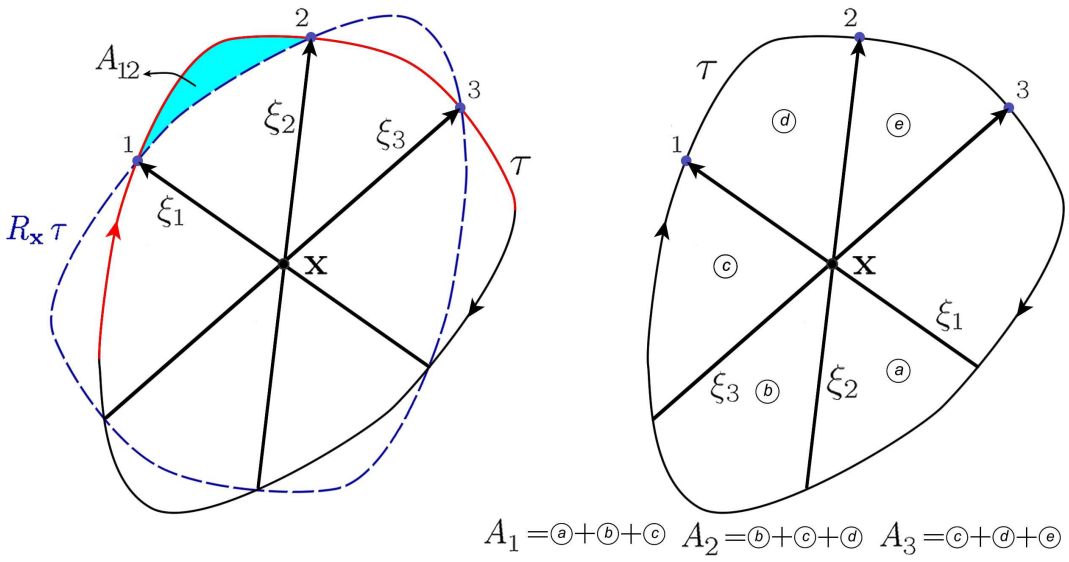

Figure 7. Stationary chords near to long-chord catastrophe of the Wigner function, displaying the compositions of the area A_j for each stationary chord. The phase difference for coalescent $\boldsymbol{\xi}_1$ and $\boldsymbol{\xi}_2$ chords is the symplectic area A_{12} limited by their tips.

Hence, the linear approximation for the amplitude in (4.2) is

$$g(z,\mathbf{x}) = \sqrt{2\hbar}\left(\zeta^{\frac{1}{4}}\Sigma I_{12} + \frac{z}{\zeta^{\frac{1}{4}}}\Delta I_{12}\right), \tag{4.5}$$

so that, the Wigner function is given by

$$W(\mathbf{x}) = 2\sqrt{2}N^2\left[\frac{\left[\frac{3}{4}A_{12}\right]^{\frac{1}{6}}\ \Sigma I_{12}\sin\left(\frac{\Sigma A}{2\hbar}\right)}{\hbar^{\frac{2}{3}}}\mathrm{Ai}\left(-\left[\frac{3A_{12}}{4\hbar}\right]^{\frac{2}{3}}\right)\right.$$
$$\left.-\frac{\Delta I_{12}\cos\left(\frac{\Sigma A}{2\hbar}\right)}{\hbar^{\frac{1}{3}}\left[\frac{3}{4}A_{12}\right]^{\frac{1}{6}}}\mathrm{Ai}'\left(-\left[\frac{3A_{12}}{4\hbar}\right]^{\frac{2}{3}}\right)\right] + W_3(\mathbf{x}). \tag{4.6}$$

We have simply added the noncaustic contribution of the third chord (4.1). Note that this procedure is quite general: The presence of even more chords, arising from indentations of the quantized curve is accomodated in the same way. (The same procedure must also be adopted to deal with the increased complexity of the chord function.) Again, as for chord function, the behaviour near the caustic is described correctly in terms of the Airy function and its derivative. Crossing the fold caustic, the coalescent chords disappear and only the additional term remains, coinciding with the simpler stationary phase approximation far form the caustic[2], although the normalization constant must be re-evaluated.

For regions where $A_{12} \gg \hbar$, we can replace the Airy function and its derivative by their asymptotic forms for large negative values, obtaining

$$W(\mathbf{x}) = \frac{4N^2}{\sqrt{2\pi\hbar}}\left[\frac{\sin\left(\frac{A_1}{\hbar}-\frac{\pi}{4}\right)}{|\{I_1^+,I_1^-\}|^{\frac{1}{2}}} + \frac{\sin\left(\frac{A_2}{\hbar}+\frac{\pi}{4}\right)}{|\{I_2^+,I_2^-\}|^{\frac{1}{2}}} + \frac{\cos\left(\frac{A_3}{\hbar}-\frac{\pi}{4}\right)}{|\{I_3^+,I_3^-\}|^{\frac{1}{2}}}\right] \tag{4.7}$$

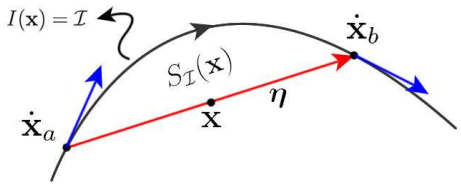

Figure 8. The area $S_{\mathcal{I}}$ for a point very close to the level curve, $I(\mathbf{x}) = \mathcal{I}$. The tips of the chord $\boldsymbol{\eta}$ evolve by the action of the Hamiltonian $I(\mathbf{x})$. As a first approximation, this evolution is linear.

which is a sum of oscillatory terms, each one with a different phase, as in (1.7). This asymptotic form is a superposition of the individual stationary phase approximations for each stationary chord.

5. Approximations for the transitional regions

The uniform approximation (3.14) is not explicitly resolved very close to the caustic, because $\mathcal{A}_{12} \to 0$ as the caustic is approached, whereas $\Sigma I^{12} \to \infty$. The classical curve can be approximated by parabolae in both the neighborhoods of the tips of the realization of $\boldsymbol{\xi}_D$. This equates the amplitude associated for each stationary point, i.e. $\Sigma I^{12} = 2\{I^+, I^-\}$ and $\Delta I^{12} \to 0$. Thus, the term of the derivative of the Airy function in (3.14) cancels near to the caustic.

To obtain an explicit expression for the transitional chord function, we start by recalling that the action variable, $I(\mathbf{x})$, can be interpreted as a Hamiltonian, such that the classical curve is a trajectory, i.e. the level curve $I(\mathbf{x}) = \mathcal{I}$. Considering $\mathbf{x}$ as the centre of a chord $\boldsymbol{\eta}$ that conects two points of the curve, $\mathbf{x}_a$ and $\mathbf{x}_b$, we obtain as a first approximation, $\mathbf{x}_b \simeq \mathbf{x}_a + \tau\dot{\mathbf{x}}_a$, if $\mathbf{x}$ is very close to this curve. Then the action can be expanded as (see Appendix B in Ref. [4])

$$\mathcal{I} - I(\mathbf{x}) \simeq \frac{1}{8}\tau^2\, \dot{\mathbf{x}}\, \mathfrak{I}_{\mathbf{x}}\, \dot{\mathbf{x}}, \tag{5.1}$$

where $\mathfrak{I}_{\mathbf{x}}$ is the Hessian matrix of I at the point $\mathbf{x}$. This quadratic Hamiltonian generates the assumed linear motion. On the other hand, the area between $\boldsymbol{\eta}$ and the curve (Fig. 8) is given by [4].

$$S_{\mathcal{I}}(\mathbf{x}) \simeq \frac{1}{12}\tau^3\, \dot{\mathbf{x}}\, \mathfrak{I}_{\mathbf{x}}\, \dot{\mathbf{x}}. \tag{5.2}$$

Thus, noticing that the centres of the realizations of $\boldsymbol{\eta}$ are $\mathbf{X}^{\pm} \equiv \pm\boldsymbol{\xi}/2$, the symplectic area $\mathcal{A}_{12}$ in Fig. 5 may be obtained as

$$\mathcal{A}_{12}(\boldsymbol{\xi}) = S_{\mathcal{I}}(\boldsymbol{\xi}/2) + S_{\mathcal{I}}(-\boldsymbol{\xi}/2) = \frac{1}{12}\left(\tau_+^3 \dot{\mathbf{X}}^+ \mathfrak{I}_{\frac{\boldsymbol{\xi}}{2}} \dot{\mathbf{X}}^+ + \tau_-^3 \dot{\mathbf{X}}^- \mathfrak{I}_{-\frac{\boldsymbol{\xi}}{2}} \dot{\mathbf{X}}^-\right) \tag{5.3}$$

where $\tau_\pm$ is the time of flight between the tips of each realization of $\boldsymbol{\eta}$, under the action of the Hamiltonian $I(\mathbf{x})$.

Recalling that $\mathbf{x}_1$ and $\mathbf{x}_2$ are the midpoints of the realizations of $\boldsymbol{\xi}$, the Poisson brackets of the action in the amplitudes in (3.14) will be given by the symplectic products,

$$\dot{\mathbf{x}}_1^+ \wedge \dot{\mathbf{x}}_1^- = \{I_1^+, I_1^-\} \simeq -\{I_2^+, I_2^-\} = \dot{\mathbf{x}}_2^- \wedge \dot{\mathbf{x}}_2^+ \tag{5.4}$$

So that defining the 'accelerations'[4, 16], $\ddot{\mathbf{x}}_1$ and $\ddot{\mathbf{x}}_2$, as

$$\ddot{\mathbf{x}}_j = \left(\dot{\mathbf{x}}_j \cdot \frac{\partial}{\partial \mathbf{x}}\right)\dot{\mathbf{x}} = \mathbf{J}\mathfrak{I}_{\mathbf{x}}\dot{\mathbf{x}}, \tag{5.5}$$

such that $\dot{\mathbf{x}}_2^+ \simeq \dot{\mathbf{x}}_1^+ + \tau_+\, \ddot{\mathbf{x}}_1^+$ and $\dot{\mathbf{x}}_1^- \simeq \dot{\mathbf{x}}_2^- + \tau_-\, \ddot{\mathbf{x}}_2^-$, we obtain

$$\{I_1^+, I_1^-\} = \frac{1}{2}\left[\tau_+\, \dot{\mathbf{X}}^-\mathfrak{I}_{\frac{\boldsymbol{\xi}}{2}}\dot{\mathbf{X}}^+ + \tau_-\, \dot{\mathbf{X}}^+\mathfrak{I}_{-\frac{\boldsymbol{\xi}}{2}}\dot{\mathbf{X}}^-\right] \tag{5.6}$$

The times τ_+ and τ_- can be found using (5.1), so that (5.3) becomes

$$\frac{3}{4}\mathcal{A}_{12}(\boldsymbol{\xi}) = \sqrt{2}\left[\frac{[\mathcal{I} - I(\frac{\boldsymbol{\xi}}{2})]^{\frac{3}{2}}}{[\dot{\mathbf{X}}^+\mathfrak{I}_{\frac{\boldsymbol{\xi}}{2}}\dot{\mathbf{X}}^+]^{\frac{1}{2}}} + \frac{[\mathcal{I} - I(-\frac{\boldsymbol{\xi}}{2})]^{\frac{3}{2}}}{[\dot{\mathbf{X}}^-\mathfrak{I}_{-\frac{\boldsymbol{\xi}}{2}}\dot{\mathbf{X}}^-]^{\frac{1}{2}}}\right]. \tag{5.7}$$

Thus, we have all the necessary ingredients to obtain the transitional form of the chord function,

$$\chi(\boldsymbol{\xi}) = \frac{e^{i\Sigma\mathcal{A}/2\hbar - i\pi/2}}{\pi^{\frac{1}{3}}h^{\frac{2}{3}}}\frac{[\tau_+^3\dot{\mathbf{X}}^+\mathfrak{I}_{\frac{\boldsymbol{\xi}}{2}}\dot{\mathbf{X}}^+ + \tau_-^3\dot{\mathbf{X}}^-\mathfrak{I}_{-\frac{\boldsymbol{\xi}}{2}}\dot{\mathbf{X}}^-]^{\frac{1}{6}}}{[\tau_+\dot{\mathbf{X}}^-\mathfrak{I}_{\frac{\boldsymbol{\xi}}{2}}\dot{\mathbf{X}}^+ + \tau_-\dot{\mathbf{X}}^+\mathfrak{I}_{-\frac{\boldsymbol{\xi}}{2}}\dot{\mathbf{X}}^-]^{\frac{1}{2}}} \times \mathrm{Ai}\left(-2^{\frac{1}{3}}\left[\frac{[\mathcal{I} - I(\frac{\boldsymbol{\xi}}{2})]^{\frac{3}{2}}}{[\dot{\mathbf{X}}^+\mathfrak{I}_{\frac{\boldsymbol{\xi}}{2}}\dot{\mathbf{X}}^+]^{\frac{1}{2}}} + \frac{[\mathcal{I} - I(-\frac{\boldsymbol{\xi}}{2})]^{\frac{3}{2}}}{[\dot{\mathbf{X}}^-\mathfrak{I}_{-\frac{\boldsymbol{\xi}}{2}}\dot{\mathbf{X}}^-]^{\frac{1}{2}}}\right]^{\frac{2}{3}}\right). \tag{5.8}$$

If the curve has a local symmetry of reflection with respect to the origin, the hessian matrices will be equal, i.e. $\mathfrak{I}_{\frac{\boldsymbol{\xi}}{2}} = \mathfrak{I}_{-\frac{\boldsymbol{\xi}}{2}}$ and the velocity vectors $\dot{\mathbf{X}}^+ = -\dot{\mathbf{X}}^-$. Here we recall that the origin depends of the chord $\boldsymbol{\xi}$, since it has been chosen to be the midpoint between the centres of its realizations on the closed curve. Thus, the transitional chord function reduces in this simple case to

$$\chi(\boldsymbol{\xi}) = \frac{e^{i\Sigma\mathcal{A}/2\hbar + i\pi}}{(2\pi)^{\frac{1}{3}}h^{\frac{2}{3}}}[\dot{\mathbf{X}}^+\mathfrak{I}_{\frac{\boldsymbol{\xi}}{2}}\dot{\mathbf{X}}^+]^{-\frac{1}{3}}\mathrm{Ai}\left(2\frac{I(\frac{\boldsymbol{\xi}}{2}) - \mathcal{I}}{[\dot{\mathbf{X}}^+\mathfrak{I}_{\frac{\boldsymbol{\xi}}{2}}\dot{\mathbf{X}}^+]^{\frac{1}{3}}}\right). \tag{5.9}$$

For a diameter $\boldsymbol{\xi}_D$, the argument of the Airy function cancels, because $I(\pm\boldsymbol{\xi}_D/2) = \mathcal{I}$, and $\Sigma\mathcal{A}/2$ is the chord area of $\boldsymbol{\xi}_D$. Thus, the transitional approximation remains finite, and at the caustic it is close to a local amplitude maximum.

We can follow a similar procedure for the Wigner function. Defining $\bar{\boldsymbol{\xi}}$, as the average between the stationary chords $\boldsymbol{\xi}_1$ and $\boldsymbol{\xi}_2$, together with the pair of phase space points, $\boldsymbol{y}^\pm = \mathbf{x} \pm \bar{\boldsymbol{\xi}}/2$, we obtain

$$W(\boldsymbol{\xi}) = \frac{4\sin\left[\frac{\Sigma\mathcal{A}}{2\hbar}\right]}{\pi^{\frac{1}{3}}h^{\frac{2}{3}}}\frac{[\tau_+^3\dot{\boldsymbol{y}}^+\mathfrak{I}_{\boldsymbol{y}^+}\dot{\boldsymbol{y}}^+ - \tau_-^3\dot{\boldsymbol{y}}^-\mathfrak{I}_{\boldsymbol{y}^-}\dot{\boldsymbol{y}}^-]^{\frac{1}{6}}}{[\tau_-\dot{\boldsymbol{y}}^+\mathfrak{I}_{\boldsymbol{y}^-}\dot{\boldsymbol{y}}^- - \tau_+\dot{\boldsymbol{y}}^-\mathfrak{I}_{\boldsymbol{y}^+}\dot{\boldsymbol{y}}^+]^{\frac{1}{2}}} \times \mathrm{Ai}\left(-2^{\frac{1}{3}}\left[\frac{[\mathcal{I} - I(\boldsymbol{y}^+)]^{\frac{3}{2}}}{[\dot{\boldsymbol{y}}^+\mathfrak{I}_{\boldsymbol{y}^+}\dot{\boldsymbol{y}}^+]^{\frac{1}{2}}} - \frac{[\mathcal{I} - I(\boldsymbol{y}^-)]^{\frac{3}{2}}}{[\dot{\boldsymbol{y}}^-\mathfrak{I}_{\boldsymbol{y}^-}\dot{\boldsymbol{y}}^-]^{\frac{1}{2}}}\right]^{\frac{2}{3}}\right). \tag{5.10}$$

Here we ommitted the contribution of the third chord in (4.6), specified by (4.1).

It is important to note that, even though the transitional approximations (5.9) and (5.10) provide simple explicit expressions for the chord function and the Wigner function, their validity is constrained to a much narrower range than the full uniform approximations in the previous sections. Indeed, whereas the latter can be extended untill the neighbourhood of some other caustic is reached (for instance, the short-chord caustic) , the asymptotic forms for the transitional approximations in this section do not describe correctly the oscillatory regime given by (3.16) or (4.7).

6. Long-chord regime for Fock states

Now we consider the excited states, $|n\rangle$, of the one dimensional harmonic oscillator whose classical manifold is a circumference centred at the origin, i.e. it has reflection symmetry. The quantization condition (2.4) for these circles defines

$$\pi(p^2+q^2) = 2\pi\hbar\left(n+\frac{1}{2}\right). \tag{6.1}$$

The exact chord function is given by [7]

$$\chi_n(\boldsymbol{\xi}) = \frac{e^{-\boldsymbol{\xi}^2/4\hbar}}{2\pi\hbar} L_n\left(\frac{\boldsymbol{\xi}^2}{2\hbar}\right), \tag{6.2}$$

where L_n is a Laguerre polynomial. For small chords, $|\boldsymbol{\xi}| \ll \hbar$,

$$\chi_{\mathcal{I}}(\boldsymbol{\xi}) \simeq \frac{1}{2\pi\hbar} J_0\left(\frac{\sqrt{2\mathcal{I}}|\boldsymbol{\xi}|}{\hbar}\right), \tag{6.3}$$

gives a good approximation for the chord function [7], where J_0, is the Bessel function of order zero. Then, the asymptotic form of the Bessel function for large values [17] leads to

$$\chi_{\mathcal{I}}(\boldsymbol{\xi}) \simeq \frac{(\sqrt{2\mathcal{I}}|\boldsymbol{\xi}|)^{-\frac{1}{2}}}{\pi\sqrt{h}} \cos\left(\frac{\sqrt{2\mathcal{I}}|\boldsymbol{\xi}|}{\hbar} - \frac{3\pi}{4}\right). \tag{6.4}$$

We can compare this result with the oscillatory regime (3.16). First, due to symmetry, the area of one chord realization is complementary to the area of the other and a simple integral gives the semiclassical phase as

$$\mathcal{A}_{\mathcal{I}}(\boldsymbol{\xi}) = 2\pi\mathcal{I} - |\boldsymbol{\xi}|\sqrt{2\mathcal{I} - \left(\frac{|\boldsymbol{\xi}|}{2}\right)^2} - 4\mathcal{I}\arcsin\left(\frac{|\boldsymbol{\xi}|/2}{\sqrt{2\mathcal{I}}}\right). \tag{6.5}$$

Moreover, symmetry equates the Poisson bracket for each chord realization, so that terms containing the derivative of Airy function will cancel. The Poisson brackets are then evaluated as

$$\{I^+, I^-\} = |\boldsymbol{\xi}|\sqrt{2\mathcal{I} - \left(\frac{|\boldsymbol{\xi}|}{2}\right)^2}, \tag{6.6}$$

so that, the uniform approximation for the chord function becomes

$$\chi_{\mathcal{I}}(\boldsymbol{\xi}) = (-1)^n \frac{\sqrt{2}N^2 \left[\frac{3}{4}\mathcal{A}_{\mathcal{I}}(\boldsymbol{\xi})\right]^{\frac{1}{6}}}{\hbar^{\frac{2}{3}}|\boldsymbol{\xi}|^{\frac{1}{2}}} \left[2\mathcal{I} - \frac{|\boldsymbol{\xi}|^2}{4}\right]^{-\frac{1}{4}} \mathrm{Ai}\left(-\left[\frac{3\mathcal{A}_{\mathcal{I}}}{4\hbar}\right]^{\frac{2}{3}}\right). \quad (6.7)$$

It follows that the asymptotic behaviour of Airy function, extrapolated for small chords is

$$\chi_{\mathcal{I}}(\boldsymbol{\xi}) = (-1)^n \frac{2N^2}{\sqrt{\hbar}} \left(\sqrt{2\mathcal{I}}|\boldsymbol{\xi}|\right)^{-\frac{1}{2}} \cos\left(\frac{\mathcal{A}_{\mathcal{I}}}{2\hbar} - \frac{\pi}{4}\right). \quad (6.8)$$

Note that, to lowest order, the argument in the Bessel function (6.3), $\sqrt{2\mathcal{I}}|\boldsymbol{\xi}|$, is one half of the complementary area to the intersection between the circle and its translation.

Thus, the asymptotic limit of the chord function for the long-chord caustic reproduces the chord function of small chords for Fock states, in an intermediary region. Furthermore, we immediately obtain the normalization constant as

$$N^2 = \frac{1}{2\pi}. \quad (6.9)$$

This is an alternative derivation to Berry's [2]. We can replace this value in (4.7) outside the caustic, where the two coalescent chords disappear, so as to recover the simpler stationary phase approximation for the Wigner function [2].

7. Discussion

We have shown that the behaviour of both the Wigner function and the chord function near a maximal chord singularity can be described by the Airy function and its derivative. Although, the latter contribution becomes negligible for points very close to the caustic, it adds an important term to the expansion of the semiclassical distributions in the oscillatory region, coinciding there with the simpler stationary phase method. The shape of the diameter-caustic is different in the phase space of centres, $\mathbf{x}$, where the Wigner function is defined, and in the space of chords, $\boldsymbol{\xi}$. In the latter case, the caustic is located on the locus of diameters, $\boldsymbol{\xi}_D$, maximal chords of the original closed complex curve. This diameter caustic is symmetrical with respect to the chord origin and it is also convex. If the assumption of convexity is relaxed, the symmetry will be preserved, because $-\boldsymbol{\xi}_D$ is also a diameter, but the simple fold caustic may then exhibit higher singularities. This is the case for the diameter-caustic viewed in the phase space of centres $\mathbf{x}_D = \mathbf{x}(\boldsymbol{\xi}_D)$. This caustic of the Wigner function has cusps even in the case of a convex quantized curve [2].

Let us summarize the behaviour of the chord function as we increase a translation in any direction: *a*) a maximum at the origin of chords; *b*) an oscillatory regime, obtained as a superposition of stationary phase terms for each chord realization; *c*) a region near to the maximal chord, i.e. the diameter $\boldsymbol{\xi}_D$, expressed in terms of the Airy function and its derivative, where the amplitude is again maximal and finally *d*) an evanescent region for chords longer than diameters (also described by the Airy functions). The only modification of this general scenario, in the case that the quantized curve is not convex,

is that there may occur previous intersections with the caustic before the evanescent region is reached. Though these interior caustics may be even more intense, in all cases there will be a local maximum in the amplitude for the interference of the state with its translation, before this decays at long distances.

We have considered only pure states, for which the phase space correlation (1.5) is given by the squared modulus of the chord function. Thus, using the asymptotic form of the uniform approximation for the chord function at the semiclassical regime, we find that, in the oscillatory region far from the caustic, the phase space correlation is approximately

$$C(\boldsymbol{\xi}) = \frac{1}{\hbar}\left[\{I_1^+, I_1^-\}^{-1} + \{I_2^+, I_2^-\}^{-1} + 2\{I_1^+, I_1^-\}^{-\frac{1}{2}}\{I_2^+, I_2^-\}^{-\frac{1}{2}} \sin\left(\frac{\mathcal{A}_{12}}{\hbar}\right)\right], \tag{7.1}$$

i.e. a pair of classical terms associated to each chord realization and a term that represents their interference. This formula corrects the semiclassical phase space correlation presented in [7], which also provides a semiclassical interpretation for the invariance of the correlation with respect to Fourier transformation. The important point is that the region near the peak in the phase space correlations, beyond which they decay, is just the squared modulus of the explicit formula (5.9), i.e. the transitional approximation for the chord function.

Acknowledgments

Partial financial support from, CNPq, FAPERJ and CAPES (brazilian agencies), as well as UNESCO/IBSP Project 3-BR-06 is gratefully acknowledged.

Appendix A. Crossed chords

Redefining $S_i = S_+$ and $S_j = S_-$ in (2.7), the phase in the integrand for the Wigner function evaluated at the point $\mathbf{x} = (p, q)$ is

$$\hbar F(Q; \mathbf{x}) = S_+(q + Q/2, I) - S_-(q - Q/2) - pQ. \tag{A.1}$$

Let q_0 and q_1 be the turning points on the closed curve, with $q_0 < q_1$. Choosing the q-axis to pass through q_0, according to Fig. A1, then at the stationary phase points, $Q = \pm\xi_q$, we have

$$S_+(q + \xi_q/2) = \int_{q_0}^{q+\xi_q/2} p_+(Q)\, dQ = a_1, \tag{A.2}$$

$$S_-(q - \xi_q/2) = \int_{q_0}^{q_1} p_+(Q)\, dQ + \int_{q_1}^{q-\xi_q/2} p_-(Q)\, dQ = a_1 + a_2 + a_3 + [-a_3 + a_4]. \tag{A.3}$$

The stationary chord, $\boldsymbol{\xi}$, is here assumed to be crossed, i.e to have both its tips on different action branches. Then, the phase becomes

$$\hbar F(\xi_q; \mathbf{x}) = a_1 - [a_1 + a_2 + a_4] - p\xi_q = -[a_2 + a_4] - p\xi_q = a - \oint p\, dq. \tag{A.4}$$

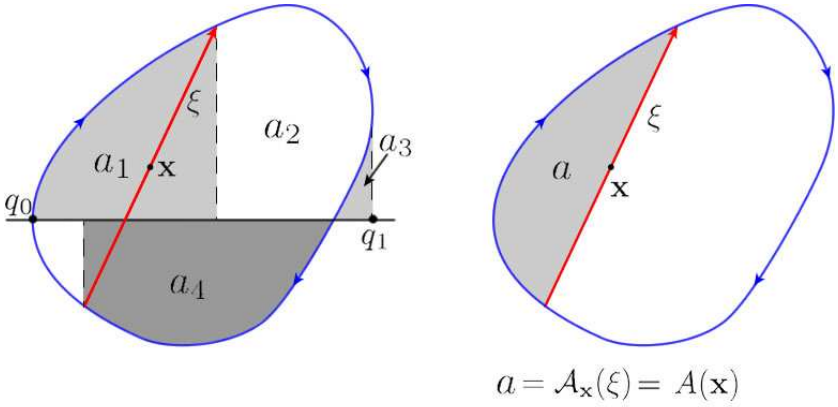

Figure A1. Phase difference between the stationary phase points for the Wigner function, evaluated at $\mathbf{x} = (p, q)$, such that the tips of its chord, $\boldsymbol{\xi} = (\xi_p, \xi_q)$, lie on different branches of the WKB function. The shaded area, $a = S_+(q + \xi_q/2) - S_-(q - \xi_q/2) - p\xi_q$,

Defining $A(\mathbf{x})$ as the area between the stationary chord and the closed curve, leads to

$$\hbar F(\xi_q; \mathbf{x}) = A(\mathbf{x}) - \oint p\, dq = A(\mathbf{x}) - 2\pi \left(n + \frac{1}{2}\right). \tag{A.5}$$

On the other hand, the phase of the integrand in (2.14) that defines the chord function for the same geometry is

$$\hbar F_\chi(Q, \boldsymbol{\xi}) = S_+(Q + \xi_q/2) - S_-(Q - \xi_q/2) - \xi_p Q. \tag{A.6}$$

The stationary points are position coordinates q, but their geometrical interpretation provides the respective momentum coordinates, p (as discussed in sec. 2). Again we denote $\mathbf{x} = (p, q)$, thus the stationary phase F_χ depends of $\mathbf{x}$ instead of only q. Choosing the q-axis in the same way as before, we obtain

$$\hbar F_\chi(\mathbf{x}, \boldsymbol{\xi}) = S_+(q + \xi_q/2) - S_-(q - \xi_q/2) - p\xi_q + p\xi_q - \xi_p q, \tag{A.7}$$

$$= S_+(q + \xi_q/2) - S_-(q - \xi_q/2) - p\xi_q + \mathbf{x} \wedge \boldsymbol{\xi} \tag{A.8}$$

Defining $\mathcal{A}_{\mathbf{x}}(\xi)$ as the symplectic area between the closed curve and the realization of $\boldsymbol{\xi}$, centred on $\mathbf{x}$, as in Fig. A1, leads to

$$\hbar F_\chi(\mathbf{x}, \boldsymbol{\xi}) = \mathcal{A}_{\mathbf{x}}(\boldsymbol{\xi}) + \mathbf{x} \wedge \boldsymbol{\xi} - 2\pi \left(n + \frac{1}{2}\right). \tag{A.9}$$

In order to implement the uniform approximations in sec. 3 and 4, we can ignore the additional term $\oint p\, dq$ in (A.5) and (A.9), because it is quantized. It should be recalled that the quantization of the closed curve implies that the areas, $A(\mathbf{x})$ and $\mathcal{A}_{\mathbf{x}}(\boldsymbol{\xi})$ and their respective complementary areas, $A'(\mathbf{x})$ e $\mathcal{A}'_{\mathbf{x}}(\boldsymbol{\xi})$, satisfy the rule

$$A(\mathbf{x}) + A'(\mathbf{x}) = \mathcal{A}_{\mathbf{x}}(\boldsymbol{\xi}) + \mathcal{A}'_{\mathbf{x}}(\boldsymbol{\xi}) = \oint p\, dq = 2\pi\hbar \left(n + \frac{1}{2}\right), \qquad n \in \mathbb{Z}. \tag{A.10}$$

Appendix B. Catastrophes for concave curves

All the geometric chords of a convex curve lie in its interior. This is a global property which is lost if perturbations of the convex curve result in smooth indentations. It is important to observe that catastrophe theory, though it is far reaching, is nonetheless only concerned with local aspects and the same goes for its quantum correspondent that deals with diffraction catastrophes. Thus, our results are in no way affected by a given chord being interior or exterior to the quantized curve.

In this Appendix we provide a simple example of the novel features that are generated by indentations. In the case of the symmetric bean-shaped torus in Fig. B1, we observe that translations of the torus, involving intersections of the concave

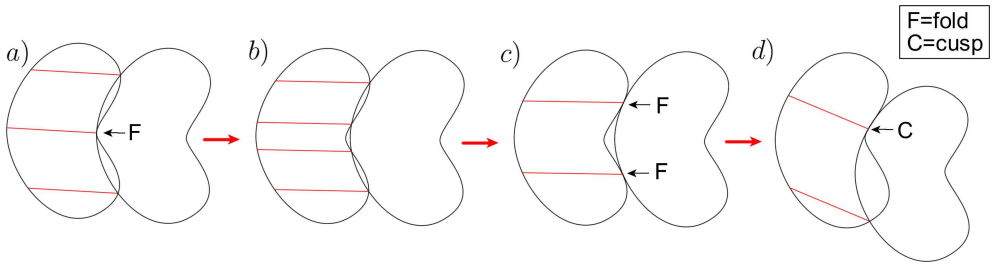

Figure B1. Catastrophes of the chord function for a concave curve. *a*) A fold caustic for the overlap of the curve with itself at the *middle point caustic* of the action S. *b*) The four chord realizations. *c*) Cusp catastrophe when the *middle chord* colasces with other one without splittes. *d*) The four realization coalesce in two pairs, obtaining two folds.

region, lead to a region with four chord realizations, Fig. B1.b. Two of these cords coalesce at a fold point, Fig. B1.a; three of them coalesce at a cusp point in Fig. B1.d and, in Fig. B1.c, we see a pair of fold points.

It is important to note that the chords for the double fold are well separated, so that they may be analyzed piecemeal within the foregoing theory. Not so the cusp points, just as in the case of the diameter caustic of the Wigner function.

For completeness we observe that a new short chord caustic also arises for the bean-torus, as shown in Fig. B2. Fig. B3 shows this, together with the diameter caustic in chord space. Both curves are symmetric about the origin. One should note that the boundary between the oscillatory region and the exterior evanescent region is still a fold line, along which the present uniform approximation is valid.

According to Thom's theorem [13], the generic structure of the diameter caustic for the chord function is not affected by further indentations, except by altering the number of cusp points and self-intersections of the fold line.

[1] Wigner E P Phys. Rev. **40** 749
[2] Berry M V, *Phil. Trans. R. Soc. Lond.* **287**, 30 (1977)
[3] Leonhardt U, *Measuring the Quantum State of Light* (Cambrigde: Cambridge University Press) (1997)
[4] Ozorio de Almeida A M, *Phys. Rep.* **295** 265 (1998)
[5] Chountasis S and Vourdas A *Phys. Rev. A.* **50** 3, pp 1794 (1998)

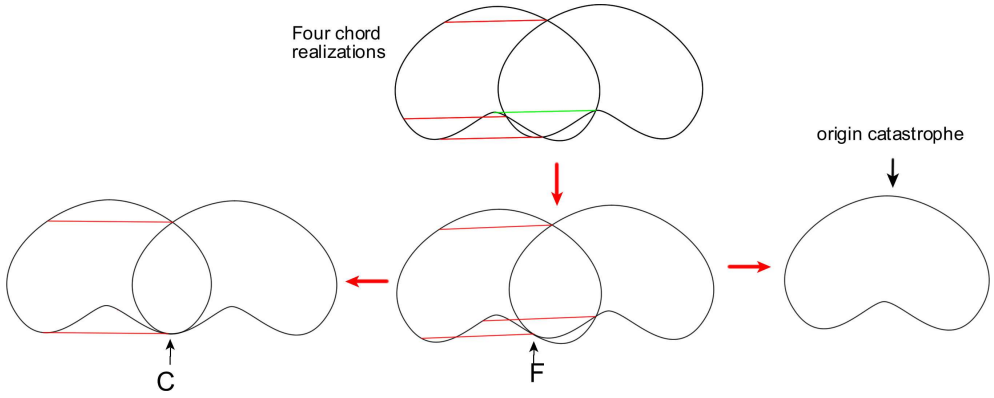

Figure B2. Construction of the short-chord catastrophe set with translations of the closed curve. The origin is a ungeneric caustic.

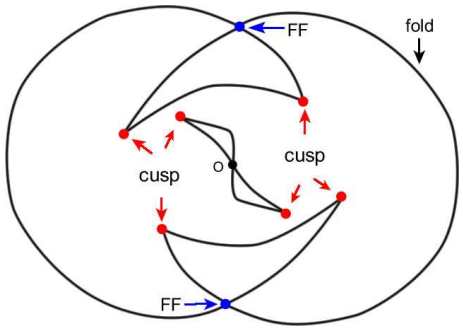

Figure B3. Catastrophes of the chord function for a concave curve in chord space. The outer curve corresponds to the long-chord caustics and the inner curve is the short-chord caustic. FF denotes a double fold caustic and O is the origin.

[6] Royer A 1977 *Phys. Rev. A* **15** 449
[7] Ozorio de Almeida A M , Vallejos R O and Saraceno M, *J. Phys. A: Math. Gen.*, **35**, 1473-1490 (2005)
[8] Ozorio de Almeida A M, *Entanglement in phase space*, *eprint* `arXiv:quant-ph/0612029` (2006) (To be published in *Theoretical Foundations of Quantum Information*, edited by Buchleitner A and Viviescas C (Lecture Notes in Physics:Springer, Berlin))
[9] Van Vleck J H, *Proc. Math. Acad. Sci.* U.S.A **14**, 178 - 188 (1928)
[10] Maslov V P and Fedoriuk M V *Semiclassical Approximation in Quantum Mechanics*(Reidel, Dordrecht) (1981) (translated from original russian edition, 1965).
[11] Ozorio de Almeida A M, *Hamiltonian Systems: Chaos and Quantization* (Cambrigde: Cambridge University Press) (1988)
[12] Gutzwiller M, *Chaos in Classical and Quantum Mechanics* (Springer, New York) (1990)
[13] Thom R, *Structural Stability and morphogenesis* (Reading, Mass: Benjamin) (1975)
[14] Chester C, Friedman B and Ursell F, *Proc. Camb. Phil. Soc. Math. Phys. Sci.* **53**, 599 (1957)
[15] Berry M V, *Adv. in Phys.* **25** 1, 1-26 (1976)
[16] Berry M V, *Proc. Soc. Roy.* **A423** 219 - 231 (1989)
[17] Abramowitz M e Stegun I, *Handbook of Mathematical Functions* (New York: Dover) (1964)